Rapid Cl /HCO 3 exchange kinetics of AE1 in HEK293 cells and hereditary stomatocytosis red blood cells

Étienne Frumence, Sandrine Genetet, Pierre Ripoche, Achille Iolascon, Immacolata Andolfo, Caroline Le van Kim, Yves Colin, Isabelle Mouro-Chanteloup, Claude Lopez

Rapid Cl^-/HCO_3^- exchange kinetics of AE1 in HEK293 cells and hereditary stomatocytosis red blood cells

Etienne Frumence,[1-5] Sandrine Genetet,[1-4] Pierre Ripoche,[1-4] Achille Iolascon,[6] Immacolata Andolfo,[6] Caroline Le Van Kim,[1-4] Yves Colin[1-4], Isabelle Mouro-Chanteloup,[1-4] and Claude Lopez[1-4*]

Author affiliations:

[1]Inserm, U665, F-75015 Paris, France; [2]Université Paris Diderot, Sorbonne Paris Cité, UMR_S665, F-75015 Paris, France; [3]Institut National de la Transfusion Sanguine, F-75015 Paris, France; [4]Laboratoire d'Excellence GR-Ex.

[5]Université de la Réunion, F-97715 Saint-Denis, France.

[6]Chair of Medical Genetics, Department of Molecular Medicine and Medical Biotechnologies, University Federico II, Naples and CEINGE-Advanced Biotechnologies, I-80145 Naples, Italy

[*]**Corresponding author** : Claude Lopez, Institut National de la Transfusion Sanguine, 6 rue Alexandre Cabanel, 75739 Paris cedex 15, France. Tel : +33 1 44 49 30 95. Fax : +33 1 43 06 50 19. E-mail : claude.lopez@inserm.fr

Author contributions:

Study concept and design: I.M.-C. and C.L.; acquisition of data: E.F., S.G., I.M.-C. and C.L.; analysis and interpretation of data: E.F., S.G., P.R., A.I., I.A., C.L.V.K., Y.C., I.M.-C. and C.L.; preparation of Figs.: E.F., S.G. and C.L.; calling of patients and collection of blood samples: A.I. and I.A.; drafting of the manuscript: E.F. and C.L.; editing and revising of the manuscript: P.R., A.I., C.L.V.K., Y.C., I.M.-C. and C.L.; final approval of the manuscript: E.F., S.G., P.R., A.I., I.A., C.L.V.K., Y.C., I.M.-C. and C.L.

Running head: Exact measurement of AE1 activity in Hst variants

ABSTRACT

Anion Exchanger 1 or Band 3 is a membrane protein responsible for the rapid exchange of chloride for bicarbonate across the red blood cell membrane. Nine mutations leading to single amino-acid substitutions in the transmembrane domain of AE1 are associated with dominant hereditary stomatocytosis, monovalent cation leaks and reduced anion exchange activity. We set up a stopped-flow spectrofluorometry assay coupled with flow cytometry to investigate the anion transport and membrane expression characteristics of wild-type recombinant AE1 in HEK293 cells, using an inducible expression system. Likewise, study of three stomatocytosis associated mutations (R730C, E758K and G796R), allowed the validation of our method. Measurement of the rapid and specific chloride/bicarbonate exchange by surface expressed AE1 showed that E758K mutant was fully active compared to WT AE1, whereas R730C and G796R mutants were inactive, reinforcing previously reported data on other experimental models. Stopped-flow analysis of AE1 transport activity in red blood cell ghost preparations revealed a 50% reduction of G796R compared to WT AE1 corresponding to a loss of function of the G796R mutated protein, in accordance with the heterozygous status of the AE1 variant patients. In conclusion, stopped-flow led to measurement of rapid transport kinetics using the natural substrate for AE1, and conjugated with flow cytometry, allowed a reliable correlation of chloride/bicarbonate exchange to surface expression of AE1, both in recombinant cells and ghosts and therefore a fine comparison of function between different stomatocytosis samples. This technical approach thus provides significant improvements in anion exchange analysis in red blood cells.

Key words : Anion exchanger 1; hereditary stomatocytosis; stopped-flow spectrofluorometry; HEK293; red blood cells

INTRODUCTION

Carbon dioxide (CO_2) is a by-product of oxidative metabolism. In human blood, CO_2 is carried through the venous system in three different ways. 5-10% is dissolved in the plasma, 5-10% is bound to hemoglobin and the remaining is converted to bicarbonate (HCO_3^-) ions by the red blood cells (RBCs). In all tissues except lung, CO_2 diffuses into RBCs where it is rapidly hydrated by carbonic anhydrase II (CAII) to form HCO_3^- and hydrogen ion (H^+) (22). HCO_3^- is very weakly lipid impermeant and is transported into the plasma in exchange for extracellular chloride (Cl^-) by the Anion Exchanger 1 (AE1, also known as Band 3), increasing the blood capacity to carry CO_2. This process called the "Chloride shift" lowers the intracellular pH (pHi), which causes a conformational change in the hemoglobin and facilitates the release of oxygen (Bohr Effect) (17). In the lung this process is reversed. Plasma HCO_3^- is transported into RBCs in exchange for intracellular Cl^- via AE1. Then HCO_3^- is dehydrated to CO_2 by CAII and diffuses out of RBCs to be expired by the lung. This process increases pHi (Fig. 1). AE1 belongs to the Solute Carrier 4A (SLC4A) family, is responsible for the Diego blood group system (2) and is the most abundant human RBC membrane protein (10^6 copies per cell) (26). It binds CAII to form the "CO_2 metabolon" and is tightly associated with the chaperone-like protein glycophorin A (GPA) (32).

AE1 has been the topic of extensive experimental transport studies, particularly in the context of transport kinetics (18). It mediates the exchange of a wide range of monovalent (nitrate, oxalate, iodide, thiocyanate) or divalent (sulfate, phosphate) anions, but chloride and bicarbonate are the physiological substrates. This Cl^-/HCO_3^- exchange across the plasma membrane occurs at the fast rate of $5x10^4$ ions per second at 37°C (16) and therefore cannot be measured easily. However, up to now most measurements on RBCs involved long-term (minutes to hours) influx or efflux of a radioactive anion by AE1 like chloride, bicarbonate, sulfate or phosphate (7), and were not adapted to rapid kinetics. Consequently, they provided data mixing both anion transport and metabolism, but no information corresponding to the physiological conditions of rapid electroneutral Cl^-/HCO_3^- exchange. AE1 activity has also been studied in HEK293 cell lines expressing transiently the recombinant protein, because it is known to be unstable in long-term expression systems (10, 31). In both chloride movement and pH change measurements, experiments lasted over several minutes, far from rapid kinetics (20, 25).

Many different mutations of human AE1 have been described. They can either be asymptomatic or can lead to hereditary hemolytic red cell diseases (spherocytosis or

stomatocytosis) (11), or hereditary distal renal tubular acidosis (1). Recently nine point mutations in the *SLC4A1* gene (L687P, D705Y, R730C, S731P, H734R, E758K, R760Q, S762R and G796R substitutions in the protein) have been reported (4, 7, 13, 14, 15, 28, 30). All these substitutions induce monovalent cation leaks in RBCs and are responsible for hereditary stomatocytosis (HSt) associated with hemolytic anemia (6). Expression of the mutated genes in *Xenopus laevis* oocytes induced abnormal Na^+ and K^+ fluxes. Intracellular pH measurements using microelectrodes, $^{36}Cl^-$ influx and $^{35}SO_4^{2-}$ efflux in oocytes, showed that HSt mutant AE1 proteins were no more functional, except for E758K and R760Q mutants that kept anion exchange activity, although cation leaks were also detected in these two variants.

In the present report, we stably expressed wild type (WT) recombinant AE1 in HEK293 cells, using a tetracycline-inducible expression system to circumvent the loss of long-term expression of the protein. Three HSt mutant AE1 were also expressed, E758K (keeping anion exchange activity), R730C and G796R (inactive), the latter being also available as RBCs from two related patients. We then set up a stopped-flow spectrofluorometry assay to investigate the rapid Cl^-/HCO_3^- exchange kinetics of normal and HSt mutant AE1. This assay is based on the detection of variations of pHi resulting from HCO_3^- influx by a fluorescent pH-sensitive dye, in the presence of HCO_3^- and Cl^- gradients. We measured this activity in HEK293 cells expressing the recombinant proteins, and also in RBC ghosts from normal individuals and HSt patients carrying the G796R mutation at the heterozygous state. Moreover, we analyzed by flow cytometry the surface expression of WT and mutant AE1 and correlated it to Cl^-/HCO_3^- exchange, allowing a reliable comparison of activities of the proteins on transfected HEK293 cells and RBCs. This study provides new insights into AE1 function in terms of kinetics, use of its natural substrate, and determination of apparent unit permeabilities for Cl^-/HCO_3^- exchange.

MATERIALS AND METHODS

Reagents. pcDNA4/TO and pcDNA6/TR (T-REx system) were purchased from Invitrogen (Leek, The Netherlands). Primers used in PCR and mutagenesis experiments were from MWG Biotech (Ebersberg, Germany). BCECF-AM [2',7'bis-(2-carboxyethyl)-5(6)-carboxyfluorescein acetoxymethyl ester] and pyranine [8-hydroxypyrene-1,3,6-trisulfonic acid] fluorescent probes, and bovine carbonic anhydrase (CA) were obtained from Sigma-Aldrich (Seelze, Germany). AE1 inhibitors DIDS [4,4 2-Diisothiocyanatostilbene-2,2 2-

disulfonic acid disodium salt] and dipyridamole were purchased from Sigma-Aldrich and DiBAC [bis(1,3-dibutylbarbituric acid) pentamethine oxonol] from Invitrogen. The mouse monoclonal antibodies anti-AE1 BRIC6 and Wr^b against the GPA/AE1 epitope were from the International Blood Group Reference Laboratory (IBGRL, Bristol, UK). The rabbit polyclonal antibody anti-AE1 was kindly provided by Dr. C. Wagner (University of Zürich, Switzerland). Secondary antibodies used in flow cytometry analysis were goat anti-mouse FITC or PE-conjugated F(ab')2 fragments from Beckman Coulter (Villepinte, France). Secondary antibodies used in confocal microscopy were Alexa Fluor 488 donkey anti-rabbit or goat anti-mouse IgG from Invitrogen.

Construction of the AE1 expression vectors and site-directed mutagenesis. Full-length cDNA encoding erythroid AE1 was amplified by PCR from the plasmid pUC18-eAE1 with addition of a Kozak sequence at its 5'end, and subcloned in the pcDNA4/TO vector. Point mutations leading to R730C, E758K, and G796R substitutions were introduced in AE1 cDNA with the QuikChange II XL site directed mutagenesis kit from Stratagene (La Jolla, CA) according to the supplier's instructions. Wild-type (WT) and mutant AE1 constructs were sequenced by the GATC company (Konstanz, Germany).

Cell culture and transfection. Human embryonic kidney (HEK) 293 cells (American Type Culture Collection, Manassas, VA) were grown in Dulbecco's modified Eagle's medium/F12/Glutamax I (Invitrogen) supplemented with 10% (v/v) fetal calf serum tetracycline-free (Dutscher, Brumath, France), nonessential amino acids 1x (Invitrogen), antibiotic-antimycotic 1x (Invitrogen), 25 mM sodium bicarbonate (Invitrogen), and 25 mM Hepes (Invitrogen). T-REx (Invitrogen) is a Tet-regulated mammalian expression system based on the binding of tetracycline (Tet) to a Tet repressor and derepression of the promoter controlling the expression of the gene of interest. HEK293 cells were first transfected with the regulatory plasmid pcDNA6/TR expressing the Tet repressor using FuGene 6 transfection reagent (Roche, Meylan, France), selected in culture medium supplemented with 5 µM blasticidin (Invitrogen) and cloned by limiting dilution. Individual clones were transiently transfected in duplicate with the pcDNA4/TO-AE1 vector, and 24 h later one half was incubated for 16 h with 1 □g/ml tetracycline (Invitrogen) (induced cells), the other half was left untreated (uninduced cells). HEK293-TR clones were analyzed by flow cytometry (see below) and one of them was selected, according to the best repression of AE1 expression in non induced cells and the best AE1 expression level in induced cells. HEK293-TR cells were

transfected with the relevant pcDNA4/TO-AE1 expression vectors and selected in culture medium supplemented with 5 μM blasticidin and 25 μM zeocin (Invitrogen). Expression of WT or mutated AE1 was induced with tetracycline and pools of cells were sorted using a Fluorescence-activated cell sorter (FACS) Influx 500 (BD BioSciences, Bedford, MA) at the Institut Jacques Monod (Paris, France). Cells exhibiting the best AE1 expression were kept. Resistant cells were analyzed by flow cytometry for AE1 expression.

Blood samples. RBCs from two patients (mother and son) carry the G796R mutation in the protein AE1 and were previously described (15). RBCs were collected in Naples (Italy) and sent to and kept frozen in the Centre National de Référence pour les Groupes Sanguins (CNRGS, Paris, France). Control RBCs were provided by the CNRGS. All samples were obtained after informed consent for the studies, according to the Declaration of Helsinki. The Institutional Review Board of the Federico II University from Naples approved the study.

Flow cytometry analysis. Expression of AE1 on HEK293 cells or RBCs and GPA/AE1 epitope on RBCs was detected using a FACSCanto II flow cytometer (BD BioSciences, Bedford, MA), after staining with the primary mouse antibodies BRIC6 (1/40) and Wr^b (1/8) (IGBRL, Bristol, UK), respectively, and secondary FITC or PE-conjugated goat anti-mouse antibody (1/100) (Beckman Coulter, Villepinte, France). The cell-surface antigen expression was quantified using as standards mouse IgG-coated calibration beads from Qifikit (Dako, Glostrup, Denmark) according to the manufacturer's instructions. The results were expressed as specific antibody-binding-capacity units that proved to be directly proportional to the number of molecules bound per cell.

Immunofluorescence confocal microscopy. As previously reported (33), HEK293 transfectants were cultured on poly-L-lysine coverslips (BD Biosciences) for 2 days before immunostaining. Cells were fixed in 4% (w/v) paraformaldehyde in PBS for 20 min and washed in PBS. Free aldehyde groups were blocked in 50 mM NH_4Cl/PBS for 10 min. Cells were then washed in PBS and permeabilized in 1% (w/v) SDS/PBS for 15 min or left untreated. After washes in PBS, non-permeabilized cells were incubated with mouse monoclonal (anti-AE1) BRIC6 (1/200), and permeabilized cells with rabbit polyclonal anti-AE1 (1/5,000) diluted in background immunostaining reducing buffer (Dako) for 1 h. Cells were washed three times in PBS/BSA (0.5%) and incubated for 1 h with Alexa Fluor 488 goat anti-mouse or donkey anti-rabbit IgG diluted in PBS/BSA (1/200). Samples were examined

by wide-field microscopy using a Nikon Eclipse TE300 inverted confocal microscope equipped with a 60× oil-immersion objective, numerical aperture 1.4.

Diameter measurements of HEK293 cells. HEK293 cell diameter was measured using a CASY TTC cell counter from Roche on an average of 1,000 cells. Four measurements were performed for each cell line.

RBC ghost preparations and diameter measurements. Preparation of RBC ghosts from normal individuals and HSt patients was carried out as previously reported (12). Briefly 200 µl of thawed blood were washed three times in PBS and resuspended in hypotonic lysis buffer (3.5 mM K_2SO_4 and 10 mM Hepes/KOH pH 7.2) for 40 min at 4°C, followed by resealing for 1 h at 37°C in resealing buffer (100 mM KCl, 10 mM Hepes/KOH pH 7.2, 1 mM $MgCl_2$ and 2 mg/ml bovine CA) containing 0.15 mM pyranine, a fluorescent pH-sensitive dye, and then washed three times in incubation buffer (100 mM KCl, 10 mM Hepes /KOH pH7.2). In some experiments resealing buffer contained various amounts of bovine CA which are detailed in Table 3. Ghost diameter measurements were performed on 300 ghosts per individual using a Zeiss Axio Observer Z1 microscope (x 1,000) equipped with an AxioCam MRm camera.

Stopped-flow analysis of Cl^-/HCO_3^- exchange. For Cl^-/HCO_3^- exchange analysis on HEK293 cells, 6 x 10^6 cells were washed twice in PBS and incubated for 30 min at 30°C in 1 ml of PBS containing 20 µM of the fluorescent pH sensitive probe BCECF-AM. Cells were washed twice in PBS, then equilibrated and resuspended in chloride buffer (130 mM NaCl, 5 mM KCl, 10 mM Hepes/KOH pH 7.2) at a concentration of 2 x 10^6 cells/ml. Cl^-/HCO_3^- exchange was measured at 30°C using a stopped-flow instrument (SFM400, Bio-Logic, Grenoble, France). Cells were rapidly mixed with an equal volume of bicarbonate buffer (110 mM Na-gluconate, 5 mM K-gluconate, 20 mM $NaHCO_3$ and 10 mM Hepes/KOH pH 7.2), generating inwardly directed 10 meq HCO_3^-/CO_2 and outwardly directed 67.5 meq Cl^- gradients. The pH-dependent fluorescence changes of BCECF were monitored at a 485 nm excitation wavelength and the emitted light was filtered with a 520 nm cut-off filter. Data from three to four time-courses were averaged and fitted to a mono-exponential function using the simplex procedure of the Biokine software package (Bio-Logic).

For Cl^-/HCO_3^- exchange analysis in RBCs, ghosts were resuspended in 3 ml of chloride buffer (100 mM KCl, 10 mM Hepes /KOH pH7.2). Then they were rapidly mixed with an equal volume of bicarbonate buffer (100 mM $KHCO_3$, 10 mM Hepes/HCl pH 7.2), generating inwardly directed 50 meq HCO_3^-/CO_2 and outwardly directed 50 meq Cl^- gradients. The pH-

dependent fluorescence changes of pyranine were monitored at a 465 nm excitation wavelength and the emitted light was filtered with a 520 nm cut-off filter.

RESULTS

Stable expression of recombinant WT and HSt mutant AE1 in HEK293 cell transfectants. HEK293 cells, although of renal origin, were previously shown to lack an endogenous expression of kAE1 (8) but not of CAII (27). As it has been shown that the generation of cell lines that constitutively overeproduce AE1 leads to cell death (30), we established permanent HEK293 cell lines with inducible expression of human AE1. HEK293 cells were primarily stably transfected with the pcDNA6/TR vector encoding the Tet repressor and then with the pcDNA4/TO vector bearing either WT AE1 cDNA or the three HSt (R730C, E758K and G796R) mutant cDNAs constructed by site-directed mutagenesis. Before analysis of HEK293 cell transfectants, AE1 production was induced with tetracycline. Flow cytometry experiments revealed AE1 at the surface of transfected cells (Fig. 2, *A* and *B*). More than 97% of the WT AE1 transfected cells expressed the protein after three weeks of zeocin selection. An apparent surface site number of about 10^5 molecules per cell was calculated from the binding capacity of the BRIC6 monoclonal antibody, using Qifikit calibration beads. As expected, no labeling could be detected on parental HEK293 cells. Mutant AE1 proteins were significantly expressed at the cell surface but at a lower level than WT AE1 (R730C, G796R, and E758K; 66%, 40% and 15% of WT molecules, respectively). Their comparison using a one-way ANOVA analysis followed by the Dunnett's multiple comparison test from GraphPad Prism software revealed statistical significance (WT AE1/R730C, $P < 0.05$; WT AE1/G796R and WT AE1/E758K: $P < 0.01$). By immunofluorescence confocal microscopy on intact and permeabilized transfected HEK293 cells (Fig. 2*C*, *left* and *right*, respectively), WT, R730C, G796R, and E758K AE1 expression was localized at the plasma membrane and also in intracellular compartments, especially for E758K mutant. These results show that WT AE1, and R730C, G796R and E758K mutants can traffic to and be stably expressed at the plasma membrane of HEK293 cells, with however a significant internal retention of the protein.

Cl^-/HCO_3^- exchange in WT and HSt mutant AE1 transfected HEK293 cells. The Cl^-/HCO_3^- exchange capacity of human AE1 proteins, stably expressed in HEK293 cells, was investigated by stopped-flow spectrofluorometry using BCECF as an intracellular pH-

sensitive probe, in the presence of inwardly directed 10 meq HCO_3^-/CO_2 and outwardly directed 67.5 meq Cl^- gradients at 30°C. This temperature (instead of the more physiological 37°C) was used to standardize experimental conditions in this study, because in RBC ghosts, kinetics at 37°C are too rapid (less than 1 s) to precisely measure Cl^-/HCO_3^- exchange (see below). Fig. 3*A* indicates the time-course of the fluorescence increase after submission of WT AE1 expressing cells to the gradients at pH 7.2. These fast kinetics allowed the calculation of alkalinization rate constants k, which correspond to the constants of the mono-exponential functions that fit to the experimental curves (Table 1). The fluorescence variation for WT AE1 cells exhibited a rapid increment corresponding to intracellular alkalinization, whereas almost no increase of fluorescence was observed in parental HEK293 cells, lacking AE1 expression (k were 0.38 ± 0.04 s^{-1} versus 0.03 ± 0.02 s^{-1}, respectively). Alkalinization in WT AE1 cells reached a plateau within about 10 s. After incubation of WT AE1 transfected cells with the anion exchanger inhibitor DIDS, Cl^-/HCO_3^- exchange was reduced at the parental HEK293 cell level (k = 0.03 ± 0.02 s^{-1}). Transport recorded in absence of DIDS is therefore totally specific of the AE1 protein. The Cl^-/HCO_3^- exchange capacity of recombinant cells expressing the HSt E758K and G796R AE1 mutants was then investigated (Fig. 3*B*). The alkalinization process was five to six times faster for AE1 WT (k = 0.38 ± 0.04 s^{-1}) compared to E758K (k = 0.07 ± 0.03 s^{-1}) and similar to parental HEK293 cells for G796R (k = 0.02 ± 0.01 s^{-1}) and R730C (k = 0.01 ± 0.01 s^{-1}) (Table 1). However, since flow cytometry analysis revealed heterogeneous expression levels of the AE1 mutants, it was essential to correlate these alkalinization rate constants to the number of molecules at the surface of HEK293 cell transfectants (Fig. 3*C*). This experiment clearly showed that the E758K mutant exhibited the same relative transport activity as WT AE1 (98% versus 100%), whereas R730C and G796R were inactive. DIDS treatment of E758K mutant also completely inhibited its Cl^-/HCO_3^- exchange capacity (k = 0.01 ± 0.01 s^{-1}), indicating the specificity of the AE1 transport activity. Determination of the number of recombinant molecules per cell was used to calculate the apparent unit permeabilities of AE1 for Cl^-/HCO_3^- at 30°C, which were equivalent for WT AE1 and E758K mutant (9.81 x 10^{-3} $\mu m^3/s$ and 11.96 x 10^{-3} $\mu m^3/s$, respectively; Table 2), thus confirming that E758K mutant was fully active.

Comparison of AE1 protein expression from control and HSt G796R mutant erythrocytes. In order to assess AE1 transport activity in RBCs from natural variants, we used blood from two normal individuals and from the two HSt patients carrying the G796R mutation in the AE1 protein, previously described (15). Evaluation by flow cytometry, using the BRIC6 antibody,

of AE1 amount in RBC membrane did not show significant differences between control and HSt patients (1.5 x 10^5 molecules per RBC), indicating neither traffic deficiency nor defective AE1 protein in G796R red cells (Fig. 4). AE1 is known to be the most abundant integral membrane protein with 10^6 copies per normal RBC; the much lower number of molecules from our result is probably attributable to steric hindrance of the BRIC6 antibody on RBCs which might prevent access to all available epitopes, as previously described (24). As GPA is tightly associated with AE1, we used an antibody against the GPA/AE1 epitope, Wr^b, to assess their co-expression in both normal and HSt patients. G796R mutant RBCs exhibited roughly the same number of molecules as control RBCs (2.8 x 10^5 versus 2.5 x 10^5 copies per cell) (Fig. 4).

Cl^-/HCO_3^- exchange in WT and G796R AE1 RBC ghosts. To measure the Cl^-/HCO_3^- exchange kinetics on RBCs, we used ghosts resealed in the presence of pyranine, a fluorescent pH-sensitive dye, and submitted to inwardly directed 50 meq HCO_3^-/CO_2 and outwardly directed 50 meq Cl^- gradients at 30°C. As mentioned above, experiments were not performed at 37°C, because anion exchange lasts much less than 1 s at this temperature, precluding an accurate determination of alkalinization rate constants. RBCs contain high levels of cytosolic carbonic anhydrase I (CAI) that is removed during the ghost preparation. They also harbor 10^6 copies of CAII directly bound to the carboxyl-terminal tail of membrane AE1 (22). This interaction is weak and pH dependent, CAII therefore can be readily removed during membrane ghost preparation, precluding any control of the CAII left amount. Indeed, our first stopped-flow experiments generated great variations of alkalinization rate constants from one ghost preparation to the other, for a same individual (not shown). WT RBC ghosts were therefore resealed in the presence of varying quantities of bovine CA and tested for Cl^-/HCO_3^- exchange by stopped-flow analysis (Table 3). CA clearly appeared to be rate-limiting to AE1 transport activity measurement since the highest alkalinization rate constant was recorded with ghosts resealed in the presence of 2 mg/ml CA ($k = 4.87 \pm 0.56\ s^{-1}$). pHi variations inside ghosts were only dependent on transmembrane Cl^-/HCO_3^- exchange at this CA concentration, all the following experiments were therefore performed under this condition. A preliminary optimization of stopped-flow methodology on RBC ghosts showed that modifications of either HCO_3^- or Cl^- gradients did not significantly alter alkalinization rate constants, whereas the amplitude of alkalinization was directly proportional with the Cl^- gradient only (not shown). Consequently, although Cl^-/HCO_3^- exchange is measured indirectly by pHi variations generated by HCO_3^- influx, Cl^- efflux actually reflects AE1 activity. Analysis of the HSt

variant activity (Fig. 5*A* and Table 4) indicated that the alkalinization process was two to three times faster in WT ghosts than in ghosts carrying the G796R mutation (k were 4.87 ± 0.56 s^{-1} versus 1.86 ± 0.17 s^{-1}) and lasted only 1s and 2 to 3 s, respectively. Since WT AE1 and G796R AE1 were expressed at the same level, correction of activity for surface expression of the protein was not necessary. Recorded k constants thus directly indicate around 60% reduction of activity of G796R ghosts compared to WT ghosts (Fig. 5*B*). Apparent unit permeability (p'_{unit}) for Cl^-/HCO_3^- was 1.7 fold lower for G796R AE1 compared to WT AE1 (2.04 x 10^{-3} $\mu m^3/s$ versus 3.49 x 10^{-3} $\mu m^3/s$) (Table 2). Of note, diameter of G796R ghosts was slightly larger than that of WT ghosts (6.8 ± 0.50 μm versus 5.9 ± 0.35 μm, n = 600), with statistical difference (t test, $P < 0.0001$) and explained the smaller difference of p'_{unit} than of constant k between WT and mutant ghosts. This result was not surprising since macrocytosis was observed on RBCs from both patients harboring the G796R mutation (15). To ascertain that these results were directly correlated to AE1 exchange, WT and HSt ghosts were incubated with 20 μM DIDS. Cl^-/HCO_3^- exchange was abolished in both WT and HSt ghosts (k = 0.02 ± 0.01 s^{-1} versus 0.03 ± 0.01 s^{-1}) (Fig. 5 and Table 4). Similar results were obtained after incubation of WT ghosts with 100 μM dipyridamole (Dipy) (k = 0.02 s^{-1}) or 100 μM DiBAC (k = 0.04 s^{-1}), other known anion exchanger inhibitors (Table 4). Replacing Cl^- with sulfate, a poorly transported organic anion, also blocked exchange activity (not shown). After incubation with 100 μM acetazolamide (ATZ), a sulfonamide that inhibits CA enzymatic activity without direct effect on anion exchange, more than 90% of Cl^-/HCO_3^- exchange was inhibited (k = 0.33 s^{-1}), confirming the crucial role of CA in our system.

DISCUSSION

AE1, associated with CAII, is responsible in erythrocytes for efficient transport of CO_2, and its hydrated form, HCO_3^-, by exchange with Cl^-. In the vast majority of AE1 mutations, there is a deficiency of this protein which causes hereditary spherocytosis, whereas if the missense mutation brings about a variant of AE1 that is inserted in the plasma membrane, the defect is associated with dominant HSt and hemolytic anemia. In the latter situation, affected individuals have an increase in RBC membrane permeability to cations and in most cases a reduction of anion movements through AE1. Expression of the mutated genes in *Xenopus laevis* oocytes induced abnormal Na^+ and K^+ fluxes (4, 7, 13, 14, 15, 28, 29). These data were consistent with the concept that the substitutions convert the protein from an anion exchanger

into an unregulated cation channel, although, so far, no study has clearly demonstrated that the cation leaks are mediated through AE1. In addition, HSt AE1 proteins exhibited no anion exchange activity, except for E758K and R760Q mutants.

We established permanent HEK293 cells with tetracycline-inducible expression of WT and HSt mutant AE1, thereby avoiding the issue of loss of this protein in long-term expression systems. Human AE1 has already been stably expressed in HEK293 cells, using muristerone A induction on cells constitutively expressing ecdysone and retinoic acid receptors (30). However, AE1 expression level was only roughly estimated by immunoblotting and immunofluorescence, which precluded a precise correlation of activity (measured by $^{36}Cl^-$ efflux and $^{35}SO_4^{2-}$ influx) with protein expression level and a quantitative comparison of these parameters between different samples. Stewart and colleagues reported that AE1 E758K mutant surface expression in amphibian oocytes was enhanced by co-expression of GPA (29), while membrane expression of R730C mutant was not (28). These results fit to our data in the HEK293 kidney cell line lacking erythroid proteins such as GPA, since E758K mutant was expressed in significant lesser amounts than R730C mutant (Newman-Keuls multiple comparison test, $P < 0.05$). Induced expression of AE1 in our system was nevertheless sufficient for exploring its transport activity without co-expression of exogenous GPA.

The Cl^-/HCO_3^- exchange through AE1 across the plasma membrane is very rapid. We could observe by stopped-flow spectrofluorometry a rapid intracellular alkalinization corresponding specifically to this exchange in HEK293 expressing WT AE1, whereas no activity was detectable in parental cells. Our results also showed that E758K mutant was fully active, as previously reported in *Xenopus* oocytes (4, 29). Indeed, although alkalinization rate constant was five to six times lower for E758K mutant than for WT AE1 (0.07 s^{-1} versus 0.38 s^{-1}), normalization of transport values with surface expression level indicated comparable relative activities (98% versus 100%) and apparent unit permeabilities (11.96 x 10^{-3} $\mu m^3/s$ versus 9.81 x 10^{-3} $\mu m^3/s$) of both E758K mutant and normal proteins. The defect in Cl^-/HCO_3^- transport activity of G796R and R730C mutants was not due to reduced expression or processing of the proteins to the cell surface and also corroborates their inactivity reported in *Xenopus* oocytes (4, 15, 28). The inducible system used is a valuable tool to control AE1 expression in HEK293 cells, and the heterogeneous amounts of the protein at cell surface from one sample to the other actually validated our method based on the comparison of activities.

We showed that stopped-flow methodology is also applicable to measure Cl^-/HCO_3^- exchange in RBCs, using ghost preparations from blood of normal individuals and HSt patients carrying the G796R mutation in the AE1 protein. In erythrocytes there is 20-fold more CAII activity than anion exchange activity (27), CAII is therefore not rate-limiting in physiological conditions. However, as we could not control the amount of CAII left after ghost preparation, it appeared that this enzyme was a limiting factor in our system. Thus we resealed the RBC ghosts in the presence of an excess of bovine CAII (2 mg/ml), in order to overcome this issue and allow an accurate measurement of Cl^-/HCO_3^- exchange by AE1. HSt G796R ghosts exhibited a 60% reduction of activity, however calculation of apparent unit permeabilities for Cl^-/HCO_3^- showed barely a 2-fold decrease for G796R AE1 compared to WT AE1 (2.04×10^{-3} $\mu m^3/s$ versus 3.49×10^{-3} $\mu m^3/s$). This discrepancy is explained by the higher diameter of mutant ghosts than that of WT ghosts, which raises the p'_{unit} value of G796R protein. This result also strengthens our findings that an accurate comparison of activity between samples not only depends on alkalinization rate constant measurement, but also on the surface expression level of AE1 (as seen above for HEK293 cells), as well as the size of the cells or RBC ghosts harboring these proteins. An approximate 50% reduction of AE1 activity in G796R ghosts was expected since this mutation is present in the heterozygous state on HSt RBCs (15), and we showed here that G796R AE1 mutant protein is inactive in HEK293 transfectants, as previously reported using pHi measurements in oocytes (4, 15). Apparent permeability in WT ghosts for Cl^-/HCO_3^- at 30°C (4.79 μm/s) is close to permeability for Cl^- measured at 38°C in RBCs (5 μm/s) at the same pH 7.2 (5). Although HEK293 cells and RBC ghosts are not comparable, since RBCs contain neither a nucleus nor the different organelles found in all other mammalian cells, WT AE1 exhibited the same range of apparent unit permeability for Cl^-/HCO_3^- in both cell systems (9.81×10^{-3} $\mu m^3/s$ and 3.49×10^{-3} $\mu m^3/s$, respectively). Even though the number of AE1 molecules at plasma membrane is underestimated because of steric hindrance of BRIC6 antibody on RBCs (24) and most probably on HEK293 cells too, the calculated permeabilities indicate that AE1 activity measurements lead to reliable results in both cell systems. We found about two times more AE1 molecules on RBCs using Wr^b antibody, it is thus required to always use the same monoclonal antibody to establish an accurate comparison of transport activities.

Taken together, the data reported here show that stopped-flow spectrofluorometry is a powerful technique to investigate the rapid transport kinetics of AE1 on both stably

transfected HEK293 cells and RBC ghosts, using the natural substrate of the protein, Cl^-/HCO_3^-. Moreover, conjugated with flow cytometry, this methodology allows for the first time a precise correlation of fast Cl^-/HCO_3^- exchange to surface expression of AE1, and therefore a fine comparison of activity between different samples. It sheds new light on the anion transport features in red blood cells presenting pathological alterations associated with AE1 abnormalities. For example, Cl^-/HCO_3^- exchange function can be potentially studied for any other AE1 mutant and in RBCs exhibiting pathologies such as AE1 clustering and/or modifications of tyrosine phosphorylation in sickle cell disease (9, 19), in G6PD deficiency (21) and senescent RBCs (3). Regulation of AE1 activity will also be assessed in stomatin-deficient RBCs since a physical link between stomatin and AE1 has recently been demonstrated (23). These future investigations will hopefully lead to the development of a new diagnosis tool for several red cell pathologies by measurement of AE1 function.

ACKOWLEDGMENTS

The authors would like to thank Nicole Boggetto (Flow cytometry platform, Institut Jacques-Monod, Paris, France) for cell sorting experiments, Julien Picot and Sylvain Bigot (Institut National de la Transfusion Sanguine, Paris, France) for flow cytometry analysis, and Eliane Véra (Centre National de Référence des Groupes Sanguins, Paris, France) for providing thawed blood samples. Funding: This work was financed by Institut National de la Transfusion Sanguine, Institut National de la Santé et de la Recherche Médicale and Université Paris Diderot. E.F. was supported by fellowships from Conseil Régional de la Réunion and Institut National de la Santé et de la Recherche Médicale. I.A. was supported by grant GGP 09044 from the Italian Telethon Foundation. Current address of E.F.: Université de la Réunion, F-97490 Sainte Clotilde, France

DISCLOSURES

No conflicts of interest, financial or otherwise, are declared by the author(s).

REFERENCES

1. **Alper SL**. Molecular physiology and genetics of Na+-independent SLC4 anion exchangers. *J Exp Biol* 212: 1672-1683, 2009.
2. **Alper SL**. Molecular physiology of SLC4 anion exchangers. *Exp Physiol* 91: 153-161, 2006.
3. **Antonelou MH, Kriebardis AG, and Papassideri IS**. Aging and death signalling in mature red cells: from basic science to transfusion practice. *Blood transfusion = Trasfusione del sangue* 8 Suppl 3: s39-47, 2010.
4. **Barneaud-Rocca D, Pellissier B, Borgese F, and Guizouarn H**. Band 3 missense mutations and stomatocytosis: insight into the molecular mechanism responsible for monovalent cation leak. *International journal of cell biology* 2011: 136802, 2011.
5. **Brahm J**. Temperature-dependent changes of chloride transport kinetics in human red cells. *The Journal of general physiology* 70: 283-306, 1977.
6. **Bruce LJ**. Hereditary stomatocytosis and cation-leaky red cells--recent developments. *Blood Cells Mol Dis* 42: 216-222, 2009.
7. **Bruce LJ, Robinson HC, Guizouarn H, Borgese F, Harrison P, King MJ, Goede JS, Coles SE, Gore DM, Lutz HU, Ficarella R, Layton DM, Iolascon A, Ellory JC, and Stewart GW**. Monovalent cation leaks in human red cells caused by single amino-acid substitutions in the transport domain of the band 3 chloride-bicarbonate exchanger, AE1. *Nature genetics* 37: 1258-1263, 2005.
8. **Bustos SP, and Reithmeier RA**. Protein 4.2 interaction with hereditary spherocytosis mutants of the cytoplasmic domain of human anion exchanger 1. *The Biochemical journal* 433: 313-322, 2011.
9. **Corbett JD, and Golan DE**. Band 3 and glycophorin are progressively aggregated in density-fractionated sickle and normal red blood cells. Evidence from rotational and lateral mobility studies. *The Journal of clinical investigation* 91: 208-217, 1993.
10. **Cordat E, Kittanakom S, Yenchitsomanus PT, Li J, Du K, Lukacs GL, and Reithmeier RA**. Dominant and recessive distal renal tubular acidosis mutations of kidney anion exchanger 1 induce distinct trafficking defects in MDCK cells. *Traffic (Copenhagen, Denmark)* 7: 117-128, 2006.
11. **Delaunay J**. The molecular basis of hereditary red cell membrane disorders. *Blood reviews* 21: 1-20, 2007.
12. **Genetet S, Ripoche P, Picot J, Bigot S, Delaunay J, Armari-Alla C, Colin Y, and Mouro-Chanteloup I**. Human RhAG ammonia channel is impaired by the Phe65Ser mutation in overhydrated stomatocytic red cells. *American journal of physiology Cell physiology* 302: C419-428, 2012.
13. **Guizouarn H, Borgese F, Gabillat N, Harrison P, Goede JS, McMahon C, Stewart GW, and Bruce LJ**. South-east Asian ovalocytosis and the cryohydrocytosis form of hereditary stomatocytosis show virtually indistinguishable cation permeability defects. *British journal of haematology* 152: 655-664, 2011.
14. **Guizouarn H, Martial S, Gabillat N, and Borgese F**. Point mutations involved in red cell stomatocytosis convert the electroneutral anion exchanger 1 to a nonselective cation conductance. *Blood* 110: 2158-2165, 2007.
15. **Iolascon A, De Falco L, Borgese F, Esposito MR, Avvisati RA, Izzo P, Piscopo C, Guizouarn H, Biondani A, Pantaleo A, and De Franceschi L**. A novel erythroid anion exchange variant (Gly796Arg) of hereditary stomatocytosis associated with dyserythropoiesis. *Haematologica* 94: 1049-1059, 2009.

16. **Jennings ML**. Structure and function of the red blood cell anion transport protein. *Annual review of biophysics and biophysical chemistry* 18: 397-430, 1989.
17. **Jensen FB**. Red blood cell pH, the Bohr effect, and other oxygenation-linked phenomena in blood O2 and CO2 transport. *Acta physiologica Scandinavica* 182: 215-227, 2004.
18. **Knauf PA**. In: *Membrane transport and renal physiology*, edited by Layton HEW, A.M. New York: Springer-Verlag, 2002, p. 85-100.
19. **Liu SC, Yi SJ, Mehta JR, Nichols PE, Ballas SK, Yacono PW, Golan DE, and Palek J**. Red cell membrane remodeling in sickle cell anemia. Sequestration of membrane lipids and proteins in Heinz bodies. *The Journal of clinical investigation* 97: 29-36, 1996.
20. **Morgan PE, Supuran CT, and Casey JR**. Carbonic anhydrase inhibitors that directly inhibit anion transport by the human Cl-/HCO3- exchanger, AE1. *Molecular membrane biology* 21: 423-433, 2004.
21. **Pantaleo A, Ferru E, Carta F, Mannu F, Simula LF, Khadjavi A, Pippia P, and Turrini F**. Irreversible AE1 tyrosine phosphorylation leads to membrane vesiculation in G6PD deficient red cells. *PloS one* 6: e15847, 2011.
22. **Reithmeier RA**. A membrane metabolon linking carbonic anhydrase with chloride/bicarbonate anion exchangers. *Blood Cells Mol Dis* 27: 85-89, 2001.
23. **Rungaldier S, Oberwagner W, Salzer U, Csaszar E, and Prohaska R**. Stomatin interacts with GLUT1/SLC2A1, band 3/SLC4A1, and aquaporin-1 in human erythrocyte membrane domains. *Biochimica et biophysica acta* 1828: 956-966, 2013.
24. **Smythe JS, Spring FA, Gardner B, Parsons SF, Judson PA, and Anstee DJ**. Monoclonal antibodies recognizing epitopes on the extracellular face and intracellular N-terminus of the human erythrocyte anion transporter (band 3) and their application to the analysis of South East Asian ovalocytes. *Blood* 85: 2929-2936, 1995.
25. **Sowah D, and Casey JR**. An intramolecular transport metabolon: fusion of carbonic anhydrase II to the COOH terminus of the Cl(-)/HCO(3)(-)exchanger, AE1. *American journal of physiology Cell physiology* 301: C336-346, 2011.
26. **Steck TL**. The band 3 protein of the human red cell membrane: a review. *J Supramol Struct* 8: 311-324, 1978.
27. **Sterling D, Reithmeier RA, and Casey JR**. A transport metabolon. Functional interaction of carbonic anhydrase II and chloride/bicarbonate exchangers. *The Journal of biological chemistry* 276: 47886-47894, 2001.
28. **Stewart AK, Kedar PS, Shmukler BE, Vandorpe DH, Hsu A, Glader B, Rivera A, Brugnara C, and Alper SL**. Functional characterization and modified rescue of novel AE1 mutation R730C associated with overhydrated cation leak stomatocytosis. *American journal of physiology Cell physiology* 300: C1034-1046, 2011.
29. **Stewart AK, Vandorpe DH, Heneghan JF, Chebib F, Stolpe K, Akhavein A, Edelman EJ, Maksimova Y, Gallagher PG, and Alper SL**. The GPA-dependent, spherostomatocytosis mutant AE1 E758K induces GPA-independent, endogenous cation transport in amphibian oocytes. *American journal of physiology Cell physiology* 298: C283-297, 2010.
30. **Timmer RT, and Gunn RB**. Inducible expression of erythrocyte band 3 protein. *The American journal of physiology* 276: C66-75, 1999.
31. **Toye AM, Banting G, and Tanner MJ**. Regions of human kidney anion exchanger 1 (kAE1) required for basolateral targeting of kAE1 in polarised kidney cells: mis-targeting explains dominant renal tubular acidosis (dRTA). *Journal of cell science* 117: 1399-1410, 2004.

32. **van den Akker E, Satchwell TJ, Williamson RC, and Toye AM**. Band 3 multiprotein complexes in the red cell membrane; of mice and men. *Blood Cells Mol Dis* 45: 1-8, 2010.
33. **Zidi-Yahiaoui N, Mouro-Chanteloup I, D'Ambrosio AM, Lopez C, Gane P, Le van Kim C, Cartron JP, Colin Y, and Ripoche P**. Human Rhesus B and Rhesus C glycoproteins: properties of facilitated ammonium transport in recombinant kidney cells. *The Biochemical journal* 391: 33-40, 2005.

FIGURE CAPTIONS

Fig. 1. The CO_2 transport in RBCs. In all tissues, carbon dioxide (CO_2) diffuses into RBCs where it is rapidly hydrated by carbonic anhydrase (CAII) to form bicarbonate (HCO_3^-) and hydrogen ion (H^+). HCO_3^- is transported into the plasma in exchange for extracellular chloride (Cl^-) by the Anion Exchanger 1 (AE1), increasing the blood capacity to carry CO_2. In lungs, plasma HCO_3^- is transported into RBCs in exchange for intracellular Cl^- via AE1. Then HCO_3^- is dehydrated to CO_2 by CAII and diffuses out of RBCs to be expired by the lung.

Fig. 2. Expression of the recombinant AE1 proteins in HEK293 cell transfectants. *A*: comparison of the AE1 surface expression by quantitative flow cytometry using BRIC6 monoclonal anti-AE1 antibody and mouse IgG-coated calibration beads Qifikit as standards. All experiments were repeated at least three times to obtain mean values (± SE). *B*: flow cytometry analysis of AE1 surface expression in HEK293 cells, using BRIC6 antibody. The *left peak* represents the non-transfected HEK293 cells and the *right peak* represents transfected cells. Percentage of positive transfected cells is indicated. *C*: immunofluorescence confocal microscopy analysis. HEK293 transfected cells were cultured on poly-L-lysine coverslips and fixed in 4% paraformaldehyde. *Left*, cells were directly labeled with mouse anti-AE1 BRIC6 and Alexa Fluor 488 goat anti-mouse IgG. *Right*, cells were permeabilized in 1% SDS before staining with rabbit anti-AE1 and Alexa Fluor 488 donkey anti-rabbit IgG. R730C exhibited similar plasma membrane and internal staining to G796R (not shown). Scale bars, 15 μm.

Fig. 3. Time course of fluorescence changes in HEK293 cells expressing WT and HSt mutant AE1. Cells loaded with the fluorescent pH-sensitive probe BCECF-AM were rapidly mixed with an equal volume of buffer containing $NaHCO_3$, generating inwardly directed 10 meq HCO_3^-/CO_2 and outwardly directed 67.5 meq Cl^- gradients. pHi-dependent fluorescence changes were monitored at a 485 nm excitation wavelength and the emitted light was filtered with a 520 nm cut-off filter, using a stopped flow spectrofluorometer. Typical time courses of fluorescence changes in HEK293 expressing WT (*A*) or mutant AE1 (*B*) are represented. In *A*,

WT AE1 HEK293 cells were incubated with the anion exchanger inhibitor DIDS (10 μM) for 30 min (*red curve*). R730C mutant exhibited similar pHi variations to G796R (not shown). Data from three time courses were averaged and fitted to a mono-exponential function using the simplex procedure of Biokine software (Bio-logic), from which alkalinization rate constants (k, s^{-1}) were calculated (see Table 1). *C*: transport activity in HEK293 cells expressing WT and mutant AE1 was represented as relative values of alkalinization rate constants correlated to the number of molecules at the surface of HEK293 cell transfectants and after subtraction of the non-transfected HEK293 cells constant. Values are means ± SE.

Fig. 4. Cell surface expression of AE1 in WT and HSt RBCs. Surface expression of AE1 by quantitative flow cytometry on two WT and two G796R RBCs, using monoclonal BRIC6 anti-AE1 and Wr^b anti-GPA/AE1 association, and mouse IgG-coated calibration beads Qifikit as standards. All experiments were repeated at least three times to obtain mean values (± SE).

Fig. 5. Time course of fluorescence changes in WT and HSt RBCs. RBC ghosts were prepared from two normal individuals and the two HSt G796R patients. Ghosts resealed in the presence of pyranine, a fluorescent pH-sensitive probe, and bovine CA at 2 mg/ml, were rapidly mixed with an equal volume of buffer containing $KHCO_3$, generating inwardly directed 50 meq HCO_3^-/CO_2 and outwardly directed 50 meq Cl^- gradients. pHi-dependent fluorescence changes were monitored at a 465 nm excitation wavelength and the emitted light was filtered with a 520 nm cut-off filter, using a stopped flow spectrofluorometer. *A* typical time courses of fluorescence changes in WT AE1 and G796R AE1 RBC ghosts incubated or not with the anion exchanger inhibitor DIDS (20 μM) for 15 min are represented. Data from three time courses were averaged and fitted to a mono-exponential function using the simplex procedure of Biokine software (Bio-logic), from which alkalinization rate constants (k, s^{-1}) were calculated (see Table IV). The time-courses were similar for both WT ghosts and both G796R ghosts, respectively. *B* transport activity in WT AE1 and G796R AE1 ghosts was represented as relative values of alkalinization rate constants. Values are means ± SE.

Table 1. *Cl^-/HCO_3^- exchange in WT and HSt mutant AE1transfected HEK293 cells*

Cell lines	Alkalinization rate constant k (s^{-1})
HEK293	0.03 ± 0.02 (5)*
WT AE1	0.38 ± 0.04 (5)
WT AE1 + DIDS†	0.03 ± 0.02 (3)
E758K	0.07 ± 0.03 (3)
E758K + DIDS†	0.01 ± 0.01 (3)
G796R	0.02 ± 0.01 (3)
R730C	0.01 ± 0.01 (3)

Values are means ± SE. **n* values in parentheses
†10 μM DIDS for 30 min.

Table 2. *Apparent permeability of AE1 for Cl^-/HCO_3^-*

	HEK293		RBC ghosts	
	WT AE1	E758K	WT AE1	G796R
Diameter, μm	17.0 ± 0.40*	16.9 ± 0.15	5.9 ± 0.35	6.8 ± 0.50
V, μm^3	2572.45	2527.32	107.54	164.64
SA, μm^2	907.92	897.27	109.36	145.27
N	100,000	15,000	150,000	150,000
k, s^{-1}	0.38	0.07	4.87	1.86
P', μm/s	1.08	0.20	4.79	2.11
p'_{unit}, $\mu m^3/s$	9.81^E-03	11.96^E-03	3.49^E-03	2.04^E-03

Diameter of HEK293 cells, around 1,000 cells measured per cell line. Diameter of ghosts, 300 ghosts measured per individual. *V*, volume; *SA*, surface area; *N*, number of AE1 copies at surface; *k*, alkalinization rate constant; *P'*, apparent permeability for Cl^-/HCO_3^- = k x V/SA, where k is the alkalinization rate constant, V is volume and SA surface area of cells or ghosts; p'_{unit}, apparent unit permeability for Cl^-/HCO_3^- at 30°C = P' x SA/N, where N is number of AE1 copies calculated using Qifikit in flow cytometry. *Values are means ± SE

Table 3. *Cl^-/HCO_3^- exchange in WT RBC ghosts in the presence of various amounts of CA*

CA* (mg/ml)	Alkalinization rate constant k (s^{-1})
0	0.73 ± 0.50 (18)†
0.1	2.58 ± 0.24 (3)
0.5	4.32 ± 0.03 (3)
1	4.58 ± 0.77 (3)
2	4.87 ± 0.56 (6)
3	4.68 ± 0.18 (4)
5	4.42 ± 0.15 (3)

Values are means ± SE.
*ghosts resealed in the presence of bovine CA.
†*n* values in parentheses.

Table 4. *Cl^-/HCO_3^- exchange in WT and G796R AE1 RBC ghosts*

RBC ghosts	Alkalinization rate constant k (s^{-1})
WT AE1	4.87 ± 0.56* (6)†
WT AE1 + DIDS‡	0.02 ± 0.01 (3)
G796R	1.86 ± 0.17 (3)
G796R + DIDS‡	0.03 ± 0.01 (3)
WT AE1 + Dipy‡	0.02 (2)
WT AE1 + DiBAC‡	0.04 (2)
WT AE1 + ATZ‡	0.33 (2)

*Values are means ± SE
†*n* values in parentheses
‡ghosts were incubated for 15 min with the appropriate inhibitor

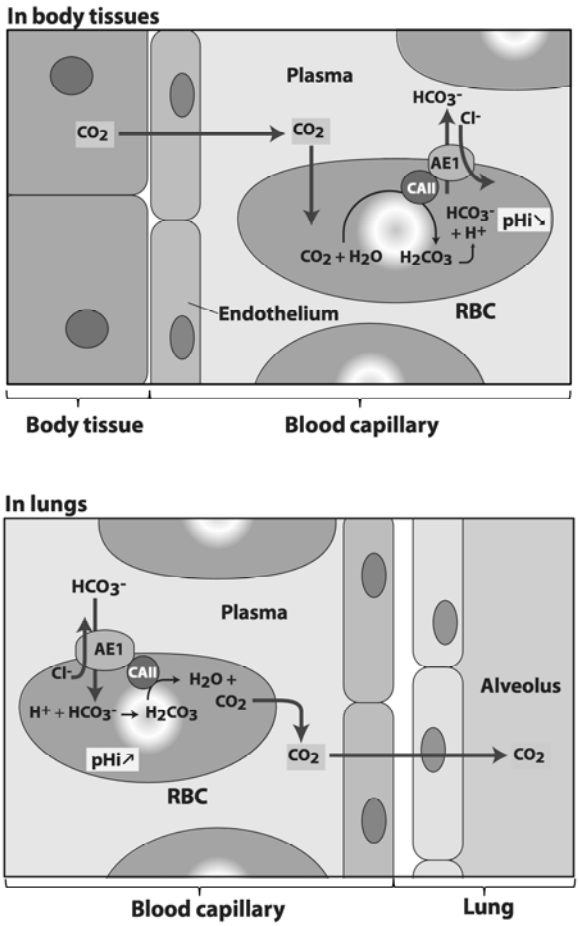
In body tissues
Plasma
CO_2
CO_2
HCO_3^-
Cl^-
AE1
CAII
HCO_3^- + H^+
pHi↘
$CO_2 + H_2O$
H_2CO_3
Endothelium
RBC
Body tissue
Blood capillary
In lungs
HCO_3^-
Plasma
AE1
Cl^-
CAII
H_2O +
CO_2
$H^+ + HCO_3^- \rightarrow H_2CO_3$
pHi↗
RBC
CO_2
Alveolus
CO_2
Blood capillary
Lung

Figure 1

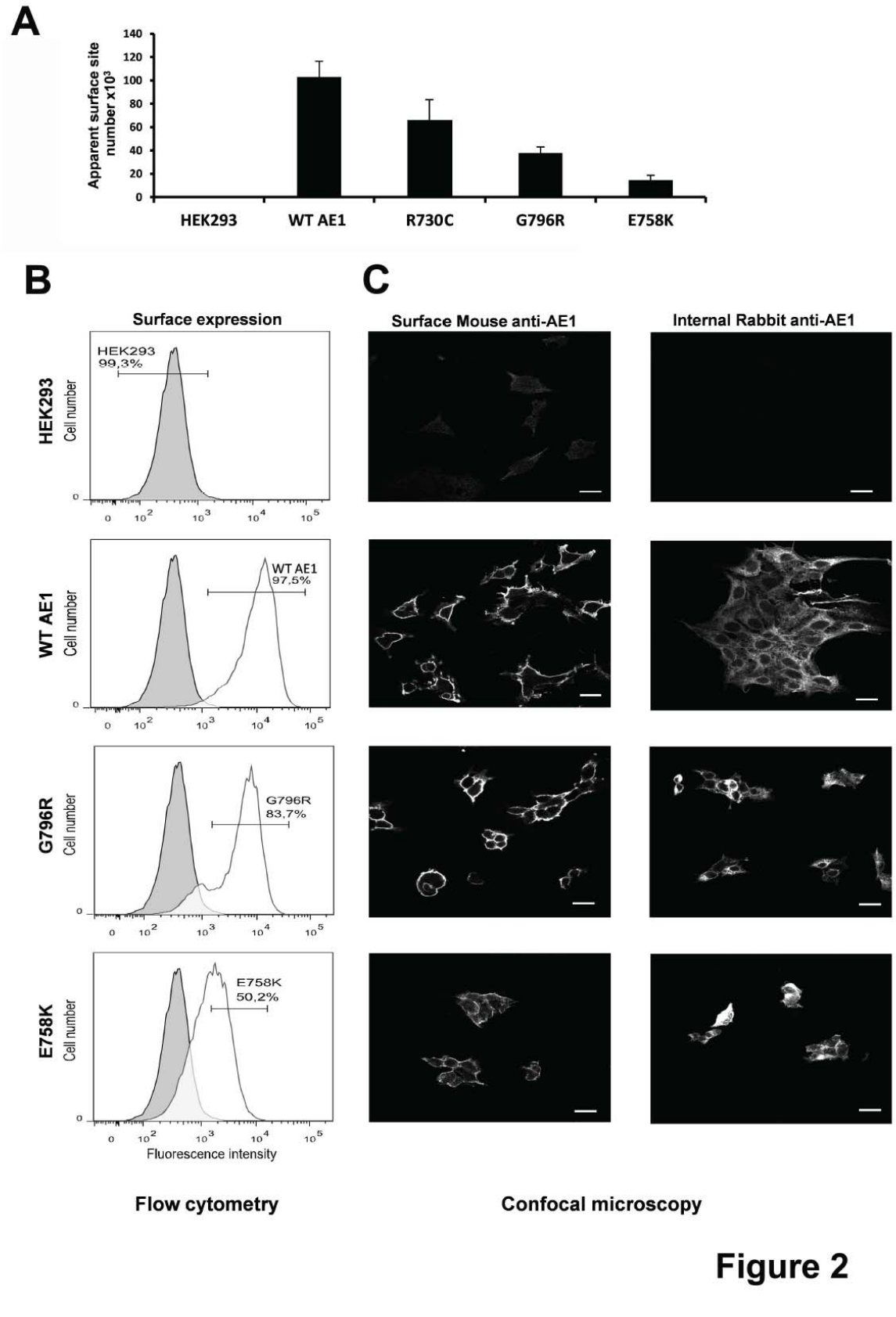
A
Apparent surface site number x10³
140
120
100
80
60
40
20
0
HEK293
WT AE1
R730C
G796R
E758K
B
C
Surface expression
Surface Mouse anti-AE1
Internal Rabbit anti-AE1
HEK293
99,3%
WT AE1
97,5%
G796R
83,7%
E758K
50,2%
Cell number
0
10²
10³
10⁴
10⁵
Fluorescence intensity
Flow cytometry
Confocal microscopy

Figure 2

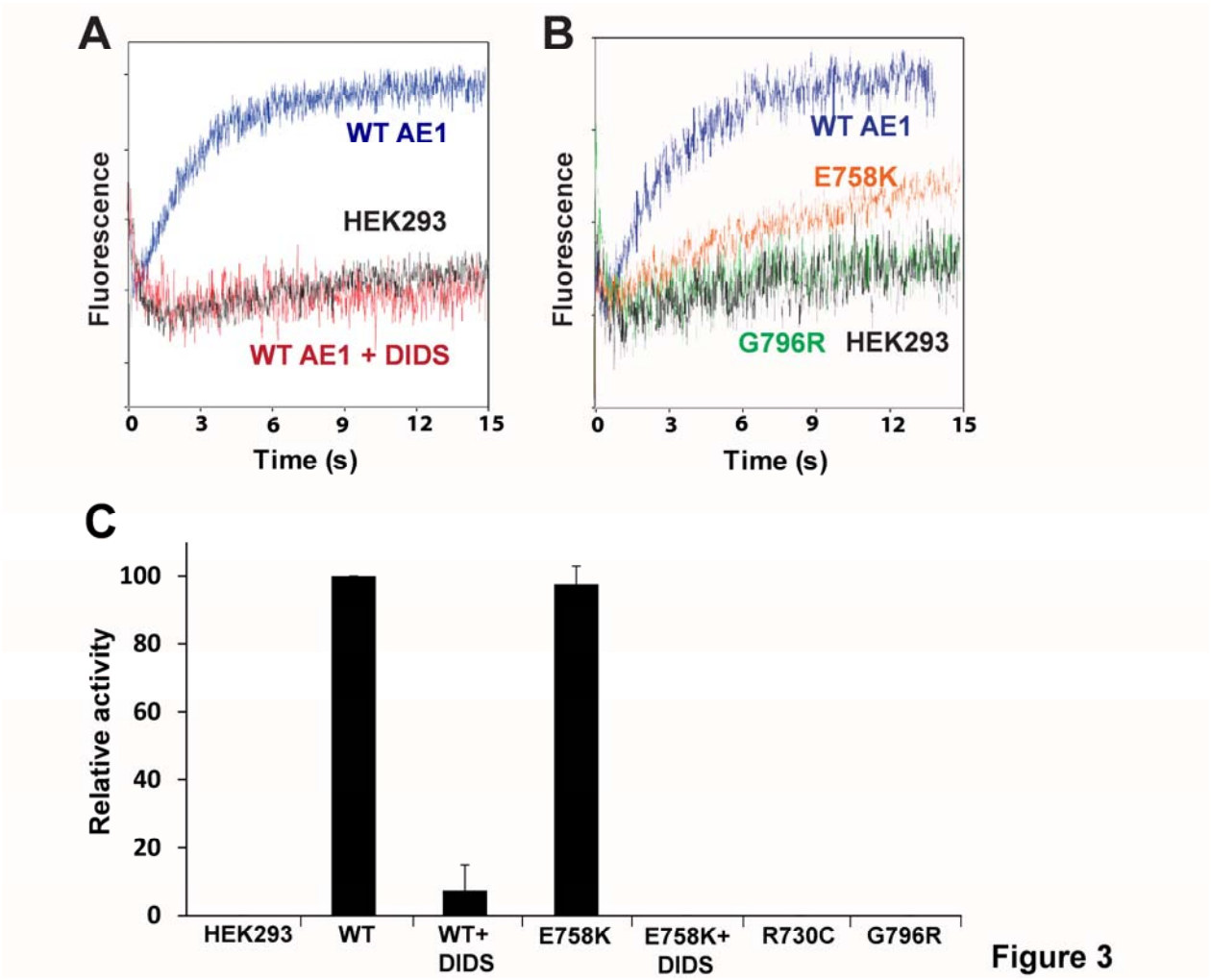
A
Fluorescence
WT AE1
HEK293
WT AE1 + DIDS
0
3
6
9
12
15
Time (s)
B
Fluorescence
WT AE1
E758K
G796R
HEK293
0
3
6
9
12
15
Time (s)
C
Relative activity
100
80
60
40
20
0
HEK293
WT
WT+ DIDS
E758K
E758K+ DIDS
R730C
G796R

Figure 3

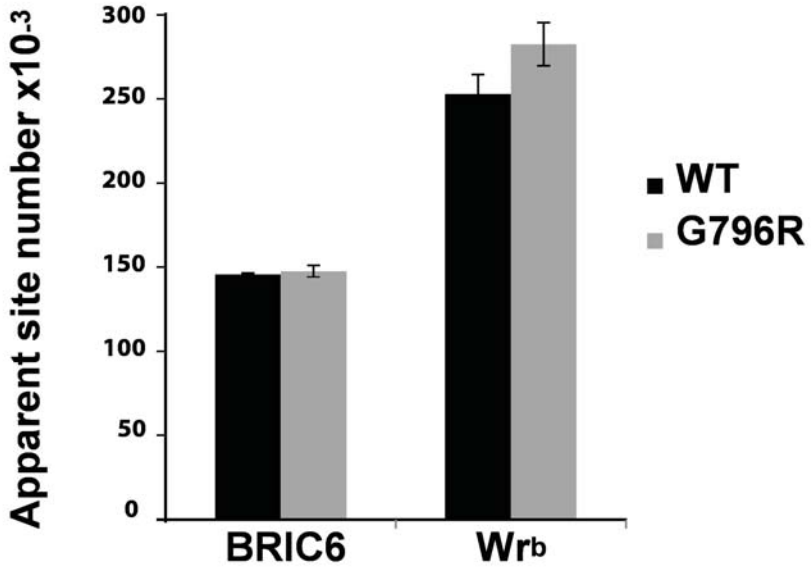
Apparent site number x10-3
300
250
200
150
100
50
0
BRIC6
Wrb
WT
G796R

Figure 4

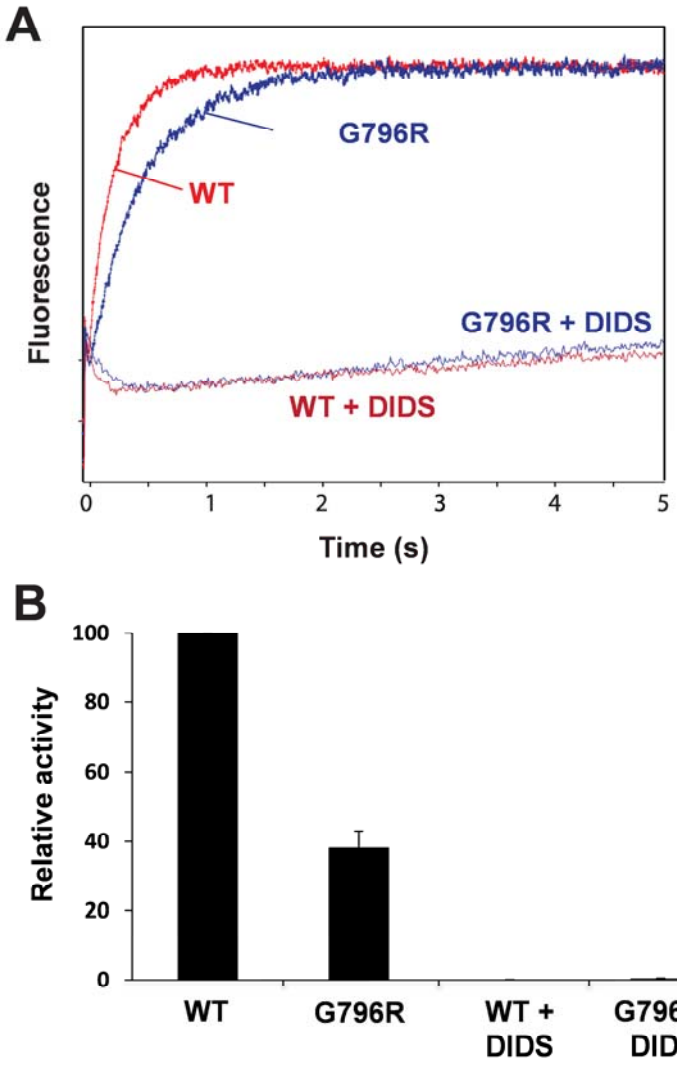
A
Fluorescence
G796R
WT
G796R + DIDS
WT + DIDS
0
1
2
3
4
5
Time (s)
B
Relative activity
100
80
60
40
20
0
WT
G796R
WT + DIDS
G796R + DIDS

Figure 5